

Techno-economics of Enhanced Geothermal Systems Across the United States Using Novel Temperature-at-Depth Maps

Mohammad J. Aljubran and Roland N. Horne

Stanford Geothermal Program, Stanford, California 94305, United States

aljubrmj@stanford.edu

Keywords: Techno-economics; Enhanced Geothermal Systems; Temperature-at-depth Maps

ABSTRACT

As geothermal technology continues to gain momentum, it becomes increasingly important for stakeholders to assess the economic feasibility of geothermal power projects when integrated into electricity markets. This study developed geographical maps demonstrating the techno-economic viability of enhanced geothermal systems (EGS) across the continental United States. Particularly, we modeled the design and operations of the upstream, midstream, and downstream system components to evaluate the levelized cost of energy (LCOE) of various EGS targets. This study integrated accurate techno-economic data including geothermal resource characteristics, capital and operational costs, temperature-at-depth maps, weather patterns, proximity to transmission lines, amongst others. Given its crucial impact on the viability of geothermal resources, we particularly developed new temperature-at-depth maps for this purpose. We also used an open-source software called Flexible Geothermal Economics Modeling (FGEM) from our previous work, to capture the effect of hourly weather variations on geothermal operations. Evaluating LCOE of EGS across depths of 1-7 km, we found that there were many sites across the continental United States where LCOE improves continuously with depth due to the favorable geothermal gradients despite the increase in drilling costs. We also found various location across depths with LCOE of less than 50 USD/MWh, which would be profitable under today's power market pricing.

1. INTRODUCTION

The global pursuit of sustainable and environmentally friendly energy sources has intensified in response to the growing concerns over climate change and declining interest in fossil fuels (Olabi et al. 2022, Holden et al. 2021). Among the diverse array of renewables, geothermal power stands out as a reliable and clean alternative, deriving its energy from the Earth's natural heat (Igwe 2021, Sharmin et al. 2023). Geothermal power has emerged as a key contender in the transition towards a greener and more resilient energy landscape, given its ability to provide consistent "baseload" power: constant, reliable, and steady supply of electricity at all times. Geothermal power is often operated under power purchase agreements (PPAs), where an operator typically earns a fixed nominal price per energy unit generated (Moradpoor et al. 2023). By signing PPAs, geothermal operators limit revenue uncertainties associated with trading in the open and volatile electricity market, especially in decarbonized grids that are significantly penetrated by intermittent resources, e.g., solar and wind (Aljubran et al. 2023). On the other hand, load-serving entities often sign geothermal PPAs as they come with continuous power availability, high capacity factors, long lifespans and stability, and environmental benefits.

As geothermal technology continues to gain momentum, it becomes increasingly important for stakeholders to assess the economic viability and profitability of geothermal power projects when integrated into electricity markets. Developers and operators are tasked with crucial decisions regarding project development, investment, and operations, all of which profoundly impact the overall success and sustainability of geothermal ventures. To make informed and strategic decisions, it is imperative to conduct a comprehensive evaluation of the techno-economics of geothermal power across geographies.

We aimed to develop geographical maps quantifying the techno-economic viability of developing EGS resources within the United States. Hence, we developed a novel temperature-at-depth model for the continental United States to improve the estimates of initial reservoir temperatures and quantify which depths are more favorable for EGS systems. Accurate techno-economic data were incorporated, including capital and operational expenditure, transmission line costs, and weather. Particularly, we modeled upstream, midstream, and downstream system components to acquire reasonable estimates of the levelized cost of electricity (LCOE). Modeling was performed for each resource at hourly resolution using an open-source tool called Flexible Geothermal Economics Modeling (FGEM), which we previously developed to enable sequential modeling of geothermal systems (Aljubran and Horne 2024).

2. MATERIALS AND METHODS

Compared to earlier studies evaluating the techno-economic feasibility of EGS resources in the United States (Augustine 2016), our work is distinct in several ways:

- We used novel temperature-at-depth maps developed using graph neural networks to provide more granular, accurate, and physically reasonable estimates of subsurface temperatures. This allowed for determining the optimal depth associated with each EGS resource location.

- Rather than using high-level tools (e.g., GETEM, GEOPHIRES), we used the FGEM tool which allows for sequential and high-resolution techno-economic modeling with various features and capabilities (Aljubran and Horne 2024). This tool was important for capturing the effect of ambient temperature on hourly power plant efficiencies and reinjection temperature.

2.1 Temperature-at-depth maps

Commonly used temperature-at-depth maps for the conterminous US were developed by the Geothermal Laboratory at Southern Methodist University (SMU) as part of a 2006 study on *The Future of Geothermal Energy*, mainly focused on assessing the potential of EGS across the US (Blackwell et al. 2006). However, the SMU maps have some limitations:

- They were developed at a gridding interval of 5 minutes (or, 0.08333°) of spatial resolution, which translates to an average spacing of about 8 km representing an area of about 64 km^2 per grid cell. A typical 250 MWe EGS plant might require about $10\text{-}20 \text{ km}^2$ of reservoir planar area to accommodate the thermal resource needed, assuming that heat removal occurs in a 0.5 km-thick region of hot rock at depth (Tester et al. 2006). With such a large areal extent, a 64 km^2 grid cell is likely to filter out many local heat anomalies. These maps also ignore EGS resources shallower than 3 km entirely, and only model depth intervals between 3-10 km (Augustine 2016).
- The analytical approach used in developing these temperature-at-depth maps requires knowledge of heat flow across the conterminous US. Note that all hydrothermal system-influenced data (very high values, i.e., generally greater than 120 mW/m^2) were excluded in this process to avoid the difficulty involved in analytically modeling regions with hot fluid up flow without overestimating temperatures at neighboring sites. This inconveniently leads to smoothing many of the most important local heat anomalies which developers would rather like to capture for economic EGS development.
- In developing such heat flow maps, a minimum curvature algorithm was used. However, such interpolation algorithms (1) are less effective with irregularly spaced data points, and (2) tend to generate smooth fits that dismiss potential heat anomalies in undersampled regions.
- SMU adopted a two-layer model where the sediment and basement contributions were captured separately. This requires knowledge of either unavailable/assumed or interpolated spatial properties across layers, such as rock thermal conductivity, measured sediment heat flow, basement heat flow, radioactive depth variable, and radioactive heat generation.

Seen in Figure 1, we developed a novel temperature-at-depth model using a graph neural network architecture tailored for interpolation tasks. Various physical quantities and data sources were collated to derive an accurate estimate of temperature-at-depth across the conterminous United States. Measurements spanned various geographic locations (Easting/Northing) and/or depth. We collected measurements for three thermal quantities: bottomhole temperature (BHT), heat flow, and rock thermal conductivity. Additionally, we allocated measurements with sufficiently high spatial resolution of other physical quantities which can be explicitly or implicitly correlated with temperature-at-depth, i.e., average surface temperature, elevation, sediment thickness, magnetic anomaly, gravity anomaly, Uranium radiation, thorium radiation, and potassium radiation. BHT measurements were acquired through direct wellbore temperature measurements at one or more depths. The collected temperature measurements could be associated with geothermal, oil & gas, groundwater, observation, and monitoring wells. After exhaustive search and curation of BHT measurements, we identified nine different raw and aggregated data sources which we integrated into a single database. These sources are SMU, Association of American State Geologists, US Geological Survey, Utah Geological Survey, Colorado Geological Survey, Maine Geological Survey, Washington State Department of Natural Resources, Geothermal Information Layer for Oregon, and Great Basin Center for Geothermal Energy. Our database included a total of 400,134 unique BHT measurements with maximum and minimum corrected BHT measurements of 0.16 and 533.71° C , respectively. Tested on 40,000 BHT data points, this temperature-at-depth model achieves accuracy of less than 3% mean percentage error.

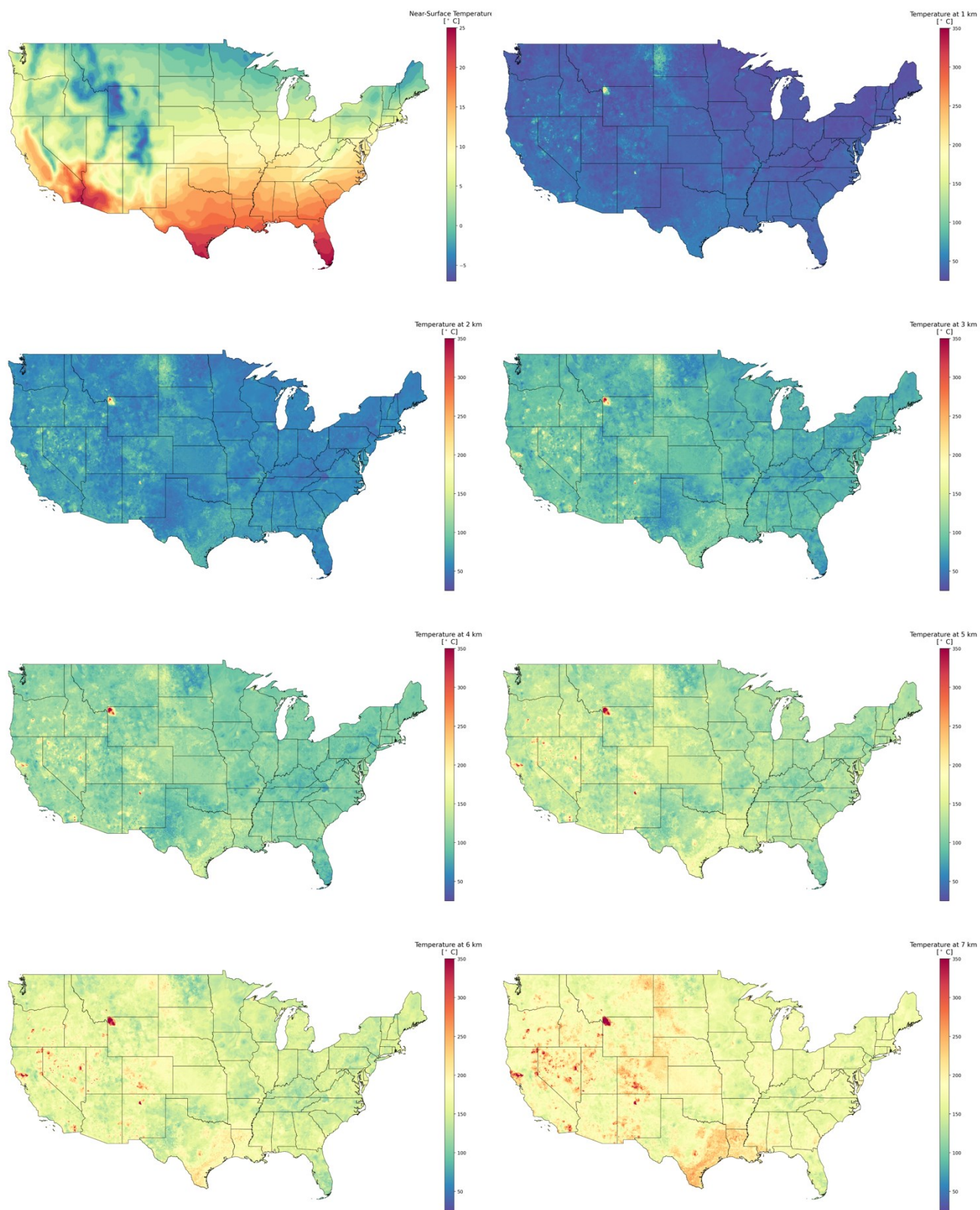


Figure 1: Temperature-at-depth model for the continental United States, spanning depths of 0-7 km with interval of 1 km.

To verify the model performance and demonstrate its utility, we evaluated the model predictions against measured temperature log data. This involved six wells from various known geothermal projects: Utah FORGE Well 58-32, Cornell's CUBO Borehole, Snake River Well

WO-2, Fallon FORGE Well 88-24, Fallon FORGE Well 61-36, and HOTSPOT Kimberly Well (Allis et al. 2018, Purwamaska et al. 2023, Podgorney 1991, Blankenship 2017, Shervais et al. 2013). In the case of temperature logs that were run soon after well drilling and completion, we applied the Harrison correction (Harrison 1983) to account for the disequibrated thermal conditions in the wellbore as a result of drilling and completion fluid circulation. It is important to note that these corrections are correlations derived based on data measured in the field before and after thermal equilibrium across wellbores. Thus, the log temperature data might be a few degrees Celsius deviant compared to the actual rock temperatures at those locations. We also included the NREL and SMU predictions to demonstrate how they differed from our model. Seen in Figure 2, our model predictions closely matched most of the temperature log data. Due to the increasing spatial sparsity of BHT measurements over depth, our model showed reasonable uncertainty magnitudes that are generally increasing with depth. We note that our model held advantages over to the NREL model, where the latter often overestimated subsurface temperatures. Additionally, unlike the SMU model whose predictions tend to frequently show static temperatures over deep intervals, our model shows increasing temperatures over depth.

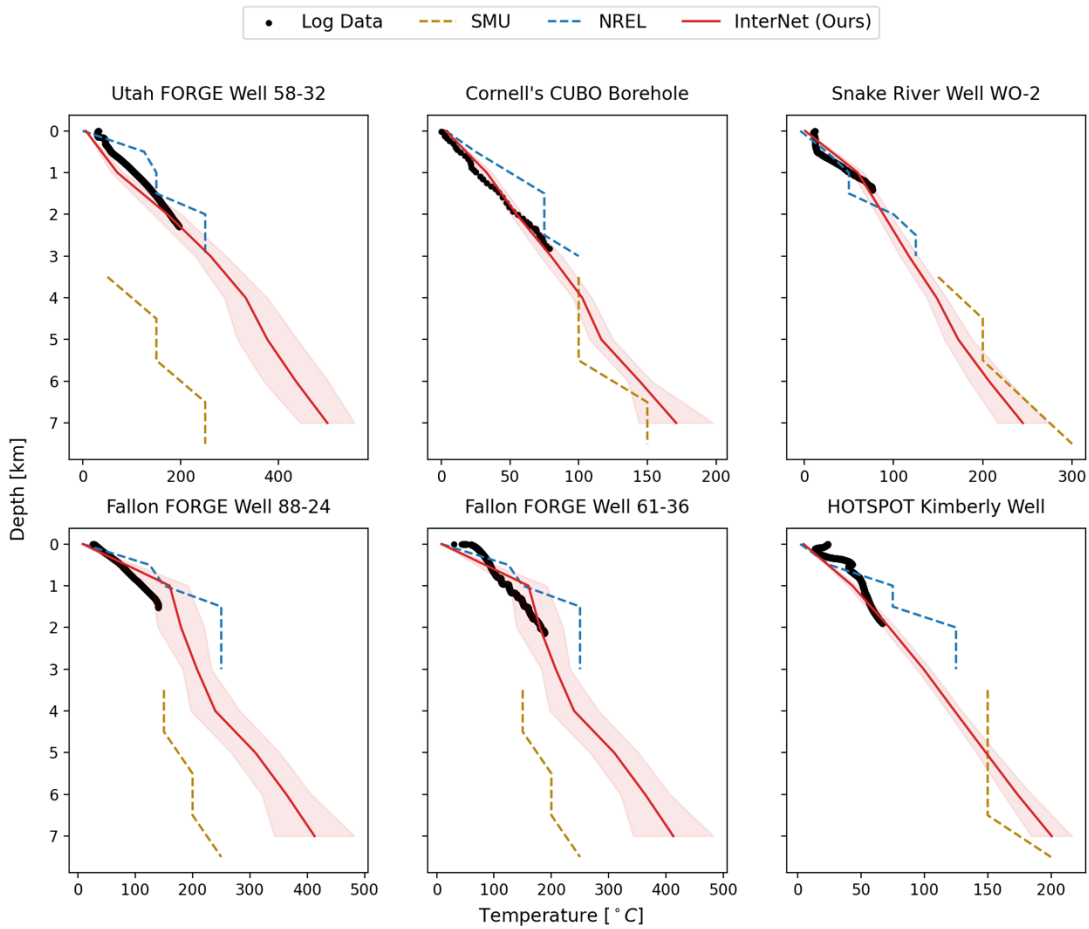


Figure 2: Verification of the proposed temperature-at-depth model using temperature log data across different locations and projects. Whereas the solid line represents the temperature-at-depth model prediction, the shaded area represents the uncertainty band, the NREL and SMU models were also visualized in dashed lines.

2.2 FGEM Tool

Developed at the Stanford Geothermal Program, FGEM is an open-source modeling tool with the overarching goal of performing comprehensive evaluation of the techno-economic feasibility and potential adaptability of baseload and flexible geothermal projects (Aljubran and Horne 2024). FGEM transcends traditional models by intertwining technical, economic, and market conditions at either high- or low-frequency timeframes. FGEM incorporates a diverse array of parameters, from geothermal resource and plant design to operational dispatch strategies and power market dynamics. This unique integration yields valuable insights into the viability of flexible geothermal power systems and their harmonization within the existing energy landscape.

The FGEM workflow requires several user inputs, including a configuration file, data files, and a dispatch strategy. These inputs undergo a thorough validation process before being used to initiate the simulation run. FGEM then performs sequential modeling through distinct modules, each modeling the techno-economic aspects of specific components within the system. These modules include the subsurface reservoir, single-phase wellbore flow dynamics and heat transfer, weather patterns, power plant performance (single flash or binary

systems), energy storage units (e.g., thermal and/or electrochemical energy storage technologies), and power market dynamics (e.g., wholesale, capacity, green energy credits, PPA). We further integrated the spatial transmission line cost into FGEM based on the existing transmission infrastructure across the continental United States. We consider an average transmission cost of 2 USD/mile-kW, which is translated to USD/kW based on the shortest distance to transmission lines, seen in Figure 3. Given their uncertainty and volatility across states, we do not quantify the techno-economic effect of topographical features and availability of transmission capacity. Nevertheless, developers need to estimate how these logistical matters may affect their project timeline and potential for attracting investments.

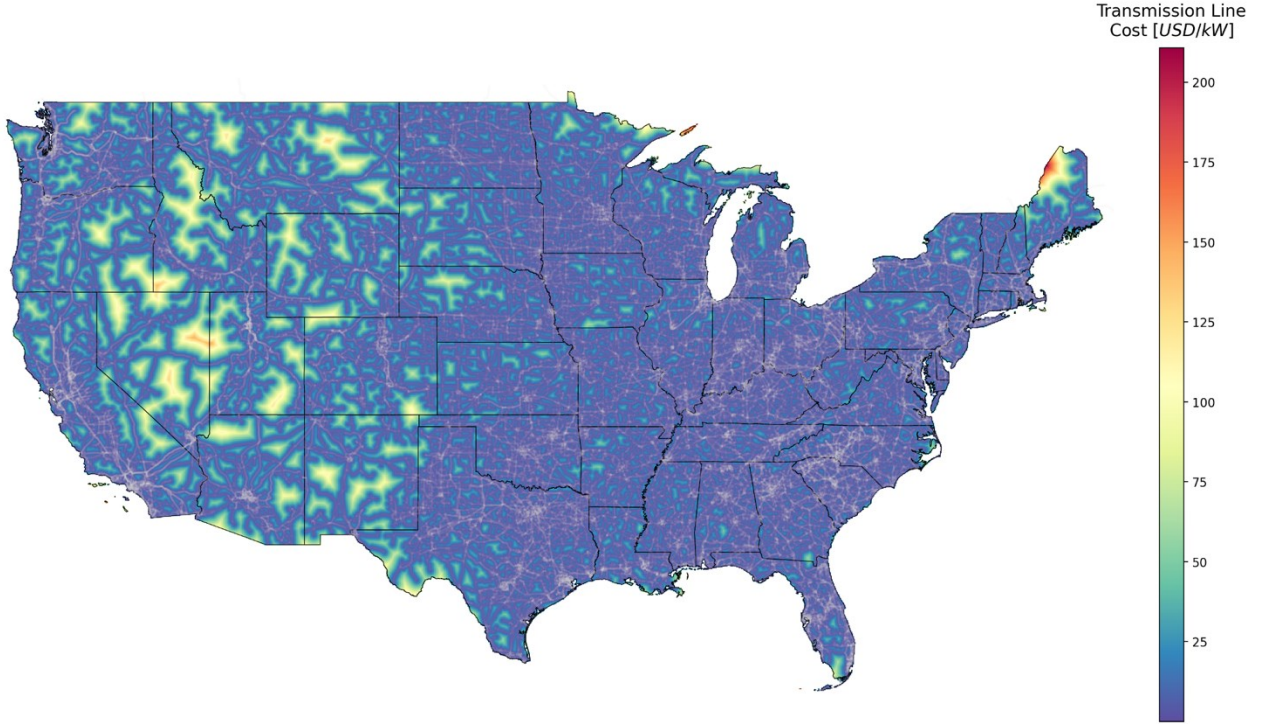


Figure 3: Spatial evaluation of the costs associated with transmission lines across the continental United States.

Evaluating the economic viability of EGS systems across seven depths (i.e., 1-7 km) at each 18 km² block within the continental US requires nearly 3.75 million simulations. We used hourly timesteps to capture the effect of weather, which makes such a task computationally intensive. Thus, to capture the subsurface EGS performance in a computationally efficient manner, we implicitly represented fractures as a single continuum (Berre et al. 2019). Particularly, we developed an analytical solution for the one-dimensional single-continuum semi-infinite transient diffusion-convection problem considering variable well flow rates and injection temperatures. As seen in Eqs 1-3, this problem can be described using the partial differential equation (PDE), and initial (IC) and boundary (BC) constraints. We used Green's function to solve this system of equations, yielding our Green's Function Model (GFM) in Eqs 4-5. Note that assuming steady-state well flow rates and injection temperatures (i.e.,) simplifies this solution to the Avdonin (1964) solution, seen in Eq. 6.

$$PDE: \frac{\partial T}{\partial t} + V(t) \frac{\partial T}{\partial x} - D \frac{\partial^2 T}{\partial x^2} = 0, \quad x, t, > 0 \quad (1)$$

$$IC: T(x, 0) = T_{res} \quad (2)$$

$$BC: T(x, t) = T_{inj}(t) \quad (3)$$

$$Definition: \bar{V}(t') = \int_0^t V(t') dt' \quad (4)$$

$$GFM \text{ Solution: } T(x, t) - T_{res} = \int_0^t \left[\frac{T_{inj}(t-\tau) - T_{res}}{\sqrt{16\pi D \tau^3}} \left[(x - \bar{V}(t)\tau) e^{\frac{(x - \bar{V}(t)\tau)^2}{4D\tau}} + (x + \bar{V}(t)\tau) e^{\frac{\bar{V}(t)x - (x + \bar{V}(t)\tau)^2}{4D\tau}} \right] \right] d\tau \quad (5)$$

$$Avdonin \text{ Solution: } T(x, t) - T_{res} = \frac{T_{inj} - T_{res}}{2} \left[\operatorname{erfc} \left[\frac{x - Vt}{\sqrt{4Dt}} \right] + e^{\frac{Vx}{D}} + \operatorname{erfc} \left[\frac{x + Vt}{\sqrt{4Dt}} \right] \right] \quad (6)$$

where $x, t, T, V, D, res, inj,$ and $erfc$ represent position, time, temperature, advective coefficient, conductive coefficient, reservoir subscript, injection subscript, and the complementary error function.

To verify the model, we compared it to the steady-state analytical solution by Avdonin (1964) as well as a numerical solution we developed in MATLAB. We particularly considered three cases: steady-state (Case-A), variable well mass flow rate (Case-B), and variable injection temperature (Case-C). Case-A is designed to be advection-dominated using a relatively large Peclet number of 31.9, with small well space-out of 300 meters, initial reservoir temperature of 205° C, fixed mass flow rate of 100 kg/s, and fixed injection temperature of 70°C. As seen in Figure 1, our GFM solution matches both the Avdonin and numerical solution very closely. Case-B is like Case-A, except that we reduced the injection cross-sectional area to induce equally diffusion-advection-dominated design, and also varied the injection temperature. Seen in Eq. 7, the injection temperature was designed to vary between 50 and 150°C annually, resembling the scenario where concentrated solar is introduced as a bottoming-cycle to geothermal power plant operations. Case-C was designed in a similar fashion to Case-B, except with steady-state injection temperature and variable well flow rates, such that flow rates were increased linearly over the project lifetime, denoted as to counteract reservoir temperature depletion. Ultimately, this would be aimed at keeping the geothermal power plant running at nameplate capacity, which could be economically favorable. Seen in Figure 5 and Figure 6, our GFM model provides an excellent fit to both Case-B and Case-C.

$$T_{inj}(t') = 50 \cdot \sin\left(\frac{2\pi}{8760 \cdot 3600} t'\right) + 100 \tag{7}$$

$$m_{prd}(t') = \frac{50}{L} t' + 50 \tag{8}$$

where $L, m,$ and prd represent the project lifetime, well mass flow rate, and producer subscript.

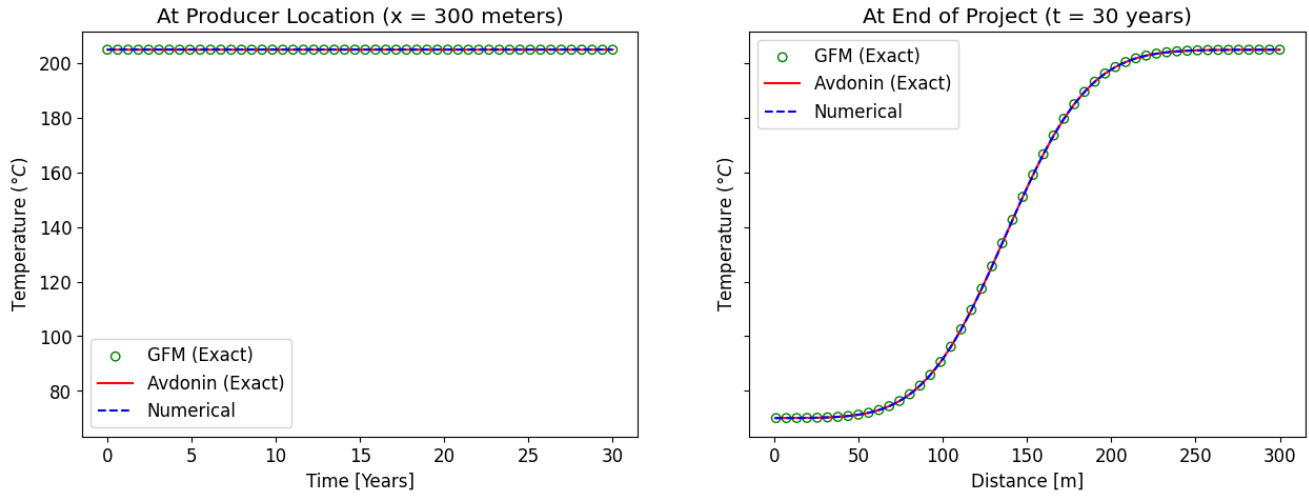


Figure 4: Comparison of our transient GFM analytical solution versus the analytical Avdonin (1964) and numerical solutions, in an advection-dominated case (Case-A) with steady-state well flow rate and injection temperature.

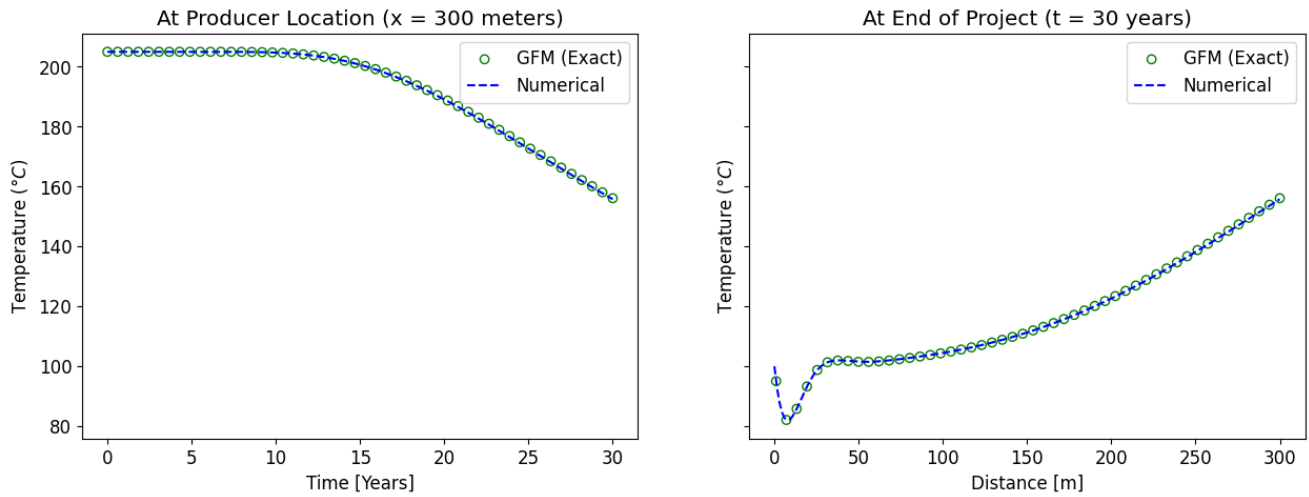


Figure 5: Comparison of our transient GFM analytical solution and numerical solution, in a design with variable injection temperature and steady-state well flow rate (Case-B).

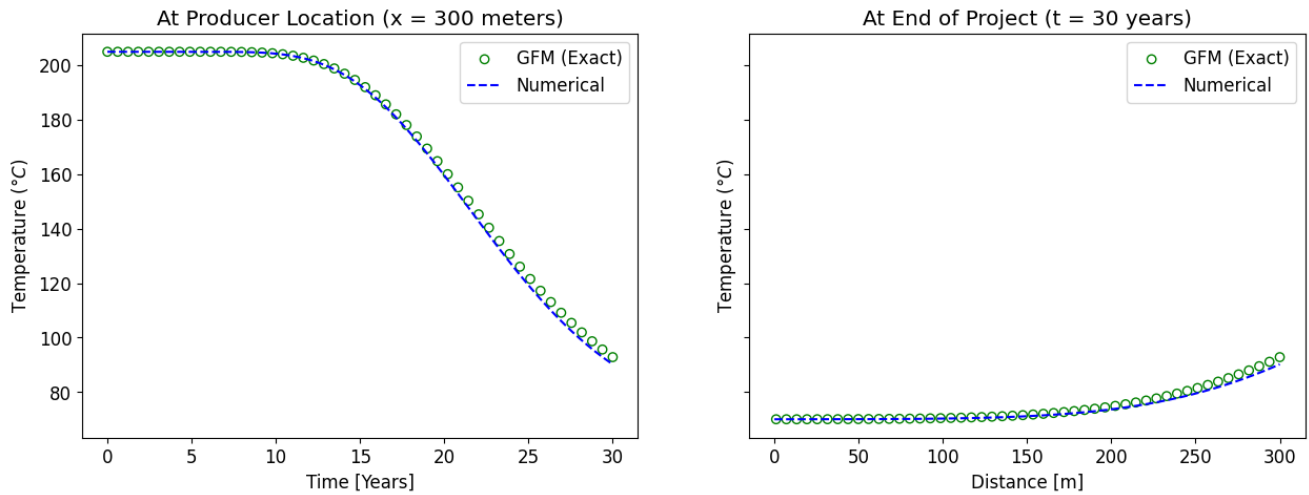


Figure 6: Comparison of our transient GFM analytical solution and numerical solution, in a design with variable injection temperature and steady-state well flow rate (Case-C).

2.3 Weather

The performance of geothermal power plants is influenced significantly by weather conditions, especially the ambient temperature. Elevated ambient temperatures can diminish the efficiency of binary cycle or flash steam systems, impacting the overall net power output. Understanding weather patterns empowers operators to fine-tune adaptable strategies for dispatching geothermal power that align with their specific conditions. Figure 7 shows the 2022 hourly ambient temperature measurements, with the national average hourly temperature highlighted in red. The pronounced fluctuations underscore the crucial role of ambient temperature as a pivotal parameter in the precise simulation and optimization of baseload and flexible geothermal operations. The techno-economic evaluation of each identified hydrothermal resource is performed using the corresponding 2022 ambient temperature records, repeated annually throughout the project lifetime.

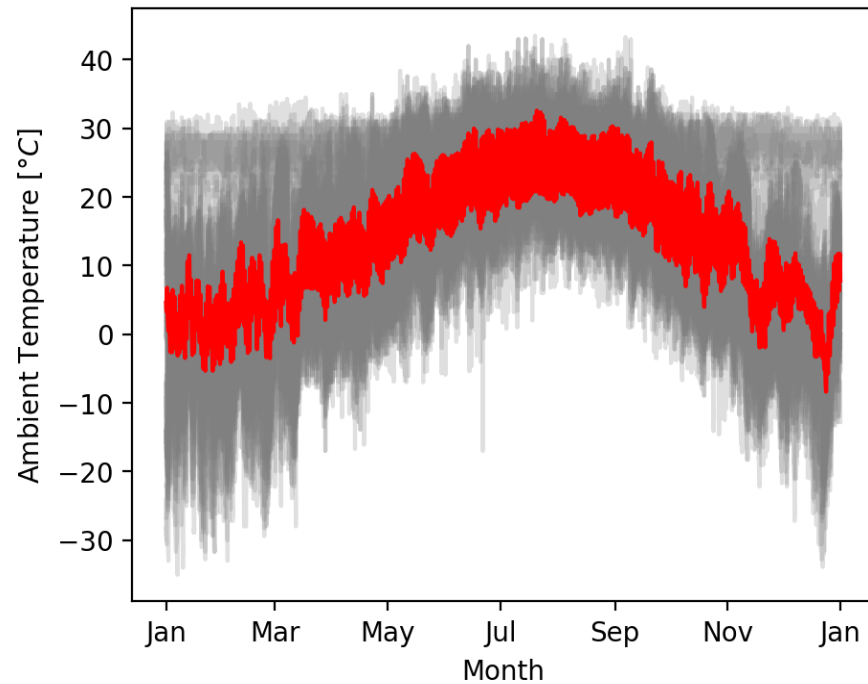


Figure 7: 2022 hourly ambient temperature for all 50 states with the mean hourly temperature plotted in red (Aljubran and Horne 2024).

3. RESULTS AND DISCUSSION

Using the described spatial quantities and EGS design components, we constructed LCOE maps for the continental United States, spanning depths of 1-7 km. Seen in Figs Figure 8Figure 9 (higher resolution LCOE maps are attached in Appendix A), we visualized the LCOE distribution across EGS systems across target reservoirs with temperatures greater than 100°C. We note that only shallower depths of 1-3 km show several opportunities with LCOE of less than 50 USD/MWh, which is competitive compared to the typical conventional geothermal PPA price of 70-100 USD/MWh. Meanwhile, deeper reservoir targets of 4-7 km concentrate experience a decreasing LCOE on average from nearly 250 to 125 USD/MWh, yet they do not display a tailed distribution with lucrative resources such as those seen in shallower depths.

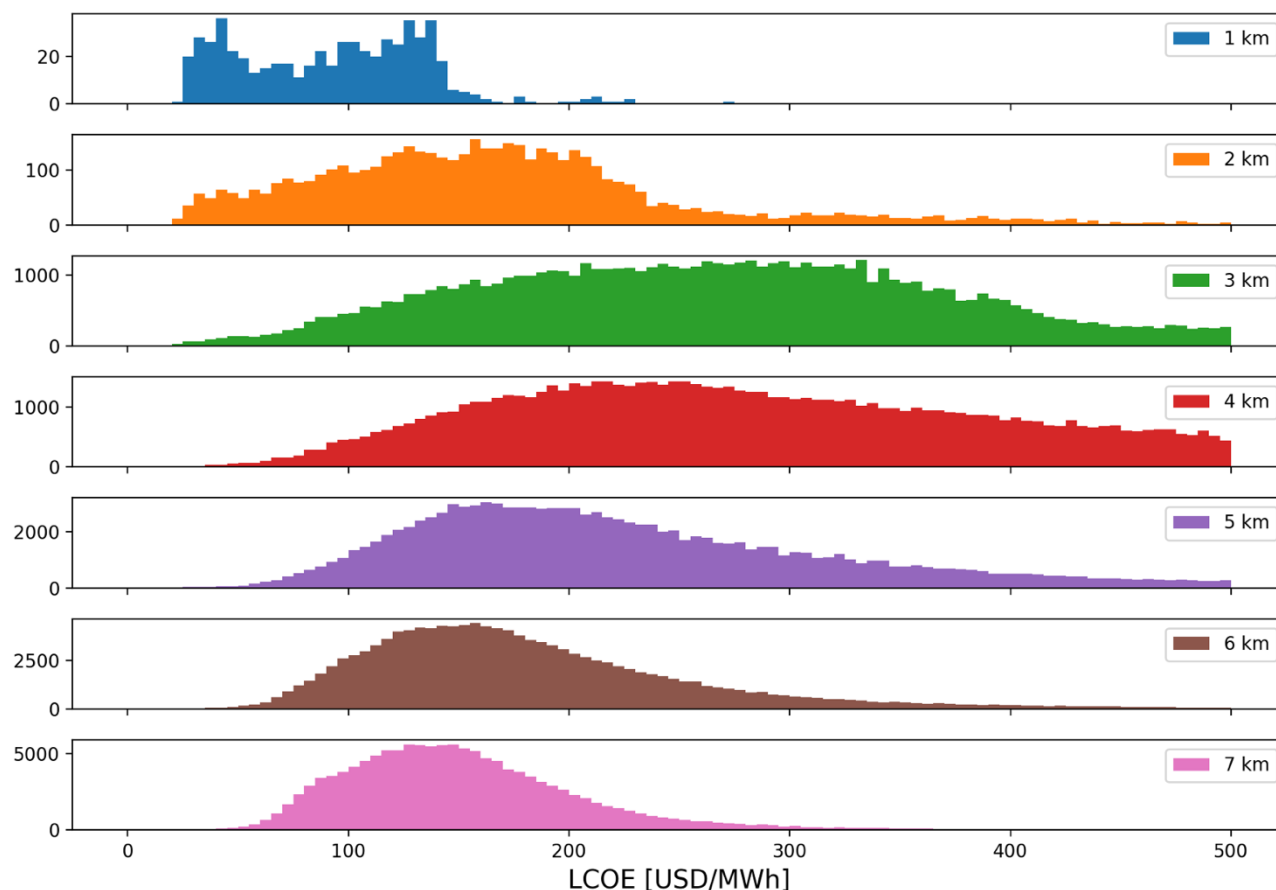


Figure 8: LCOE Histogram distribution of the performance of EGS in the continental United States. Note that this chart only includes target reservoirs with subsurface temperature of greater than 100°C.

Seen in Figure 9, the gray areas indicate economically infeasible reservoir targets with subsurface temperatures of less than 100°C. We note that target reservoirs at depth of 1 km are mostly infeasible due to their low temperatures. Moving to a depth of 2 km, we observe various sites and basins that are economically feasible. Some involve volcanos such as Yellowstone, Valdes, and Newberry, while others span various sites across the northern and western flank, such as The Geysers, the Great Basin, and Salton Sea. Upon reaching a depth of 3 km, we observe many sites with significant spatial extent that are viable with LCOE of nearly 60-100 USD/MWh. However, for those projects to be sufficiently profitable compared to other energy resources, LCOEs would have to be well below the typical conventional geothermal PPA price of 70-100 USD/MWh. Such opportunities are generally present at depths of 1-5 km which are reachable from the perspective of drilling.

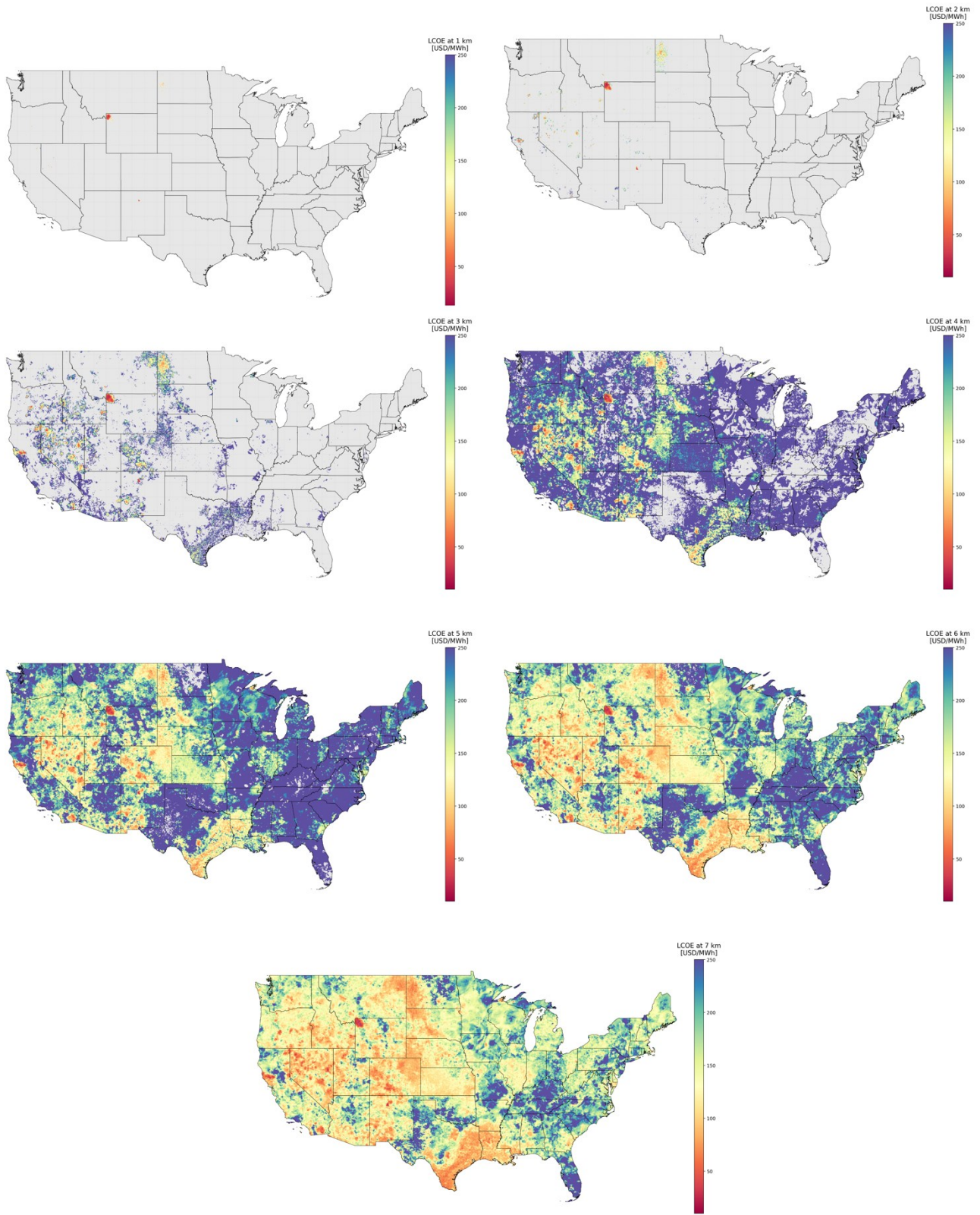


Figure 9: LCOE of EGS systems around the continental United States across depths of 1-7 km.

4. CONCLUSION

We evaluated the techno-economics of EGS projects across depths of 1-7 km in the continental United States. In this process, we developed and integrated various tools and models, such as temperature-at-depth models, analytical solution of the one-dimensional semi-infinite transient diffusion-advection problem, FGEM for sequential simulation of geothermal systems, amongst others. Using such methods, we developed LCOE maps per depth and found various locations with potential LCOE of less than 50 USD/MWh, which can be profitable in today's power markets. We also found that there are many sites across the continental United States where LCOE improves continuously with depth despite the increase in drilling expenditure due to the favorable geothermal gradients. The temperature-at-depth and LCOE maps we presented are particularly beneficial to estimating the supply curves of and developing geothermal resources across the United States.

REFERENCES

- Aljubran, M. J., and Horne, R. N.: FGEM: Flexible Geothermal Economics Modeling Tool. *Applied Energy*, 353, (2024), 122125.
- Aljubran, M. J., Volkov, O., and Horne, R. N.: Techno-Economic Modeling and Optimization of Flexible Geothermal Operations Coupled with Energy Storage. *Proceedings, 48th Stanford on Geothermal Reservoir Engineering*, Stanford University, Stanford, CA (2023).
- Allis, R., Gwynn, M., Hardwick, C., Hurlbut, W. and Moore, J.: Thermal Characteristics of the FORGE Site, Milford, Utah. *Geothermal Resources Council Transactions*, 42, (2018), 15.
- Augustine C.: Update to Enhanced Geothermal System Resource Potential Estimate. National Renewable Energy Lab, Golden, CO (2016).
- Avdonin, N. A.: Some Formulas for Calculating the Temperature Field of a Stratum Subject to Thermal Injection. *Neft'i Gaz* 3, (1964), 37-41.
- Berre, I., Florian, D., and Eirik, K.: Flow in Fractured Porous Media: A Review of Conceptual Models and Discretization Approaches. *Transport in Porous Media* 130, (2019), 215-236.
- Blackwell, D., Negraru, P., and Richards, M. C.: Assessment of the Enhanced Geothermal System Resource Base of the United States. *Natural Resources Research*, 15, (2006).
- Blankenship, D.: The Proposed Fallon FORGE Site: Phase 2 Update. Sandia National Lab, Albuquerque, NM (2017).
- Harrison, W.: Geothermal Resource Assessment in Oklahoma. Oklahoma Geological Survey, Norman, OK, (1983).
- Holden, E., Kristin L., and Rygg, B.: A Review of Dominant Sustainable Energy Narratives. *Renewable and Sustainable Energy Reviews*, 144, (2021), 110955.
- Igwe, C.: Geothermal Energy: A Review. *Int. J. Eng. Res. Technol*, 10, (2021), 655-661.
- Moradpoor, I., Syri, S., and Santasalo-Aarnio, A.: Green Hydrogen Production for Oil Refining–Finnish Case. *Renewable and Sustainable Energy Reviews*, 175, (2023), 113159.
- Olabi, A., and Abdelkareem, M.: Renewable Energy and Climate Change. *Renewable and Sustainable Energy Reviews*, 158, (2022), 112111.
- Podgorney, R.: Snake River Plain FORGE: Well Data for WO-2. USDOE Geothermal Data Repository (United States), Idaho National Lab, Idaho Falls, ID, (1991).
- Purwamaska, I., and Fulton, P.: Preliminary Constraints on Thermal Conditions within the Cornell University Borehole Observatory (CUBO). *Proceedings, 48th Workshop on Geothermal Reservoir Engineering*, Stanford University, Stanford, CA (2023).
- Sharmin, T., Khan, N., Akram, M., and Ehsan, M.: A State-of-the-art Review on for Geothermal Energy Extraction, Utilization, and Improvement Strategies: Conventional, Hybridized, and Enhanced Geothermal Systems. *International Journal of Thermofluids*, (2023), 100323.
- Shervais, J., Schmitt, D., Nielson, D., Evans, J., Christiansen, E., Morgan, L., Shanks, P., Prokopenko, A., Lachmar, T., Liberty, L., and Blackwell, D.: First Results from HOTSPOT: the Snake River Plain Scientific Drilling Project, Idaho, USA. *Scientific Drilling*, 15, (2013), 36-45.
- Tester, J., Anderson, B., Batchelor, A., Blackwell, D., DiPippo, R., Drake, E., Garnish, J., Livesay, B., Moore, M., Nichols, K., and Petty, S.: The Future of Geothermal Energy. *Massachusetts Institute of Technology*, 358, (2006), 1-3.

APPENDIX A

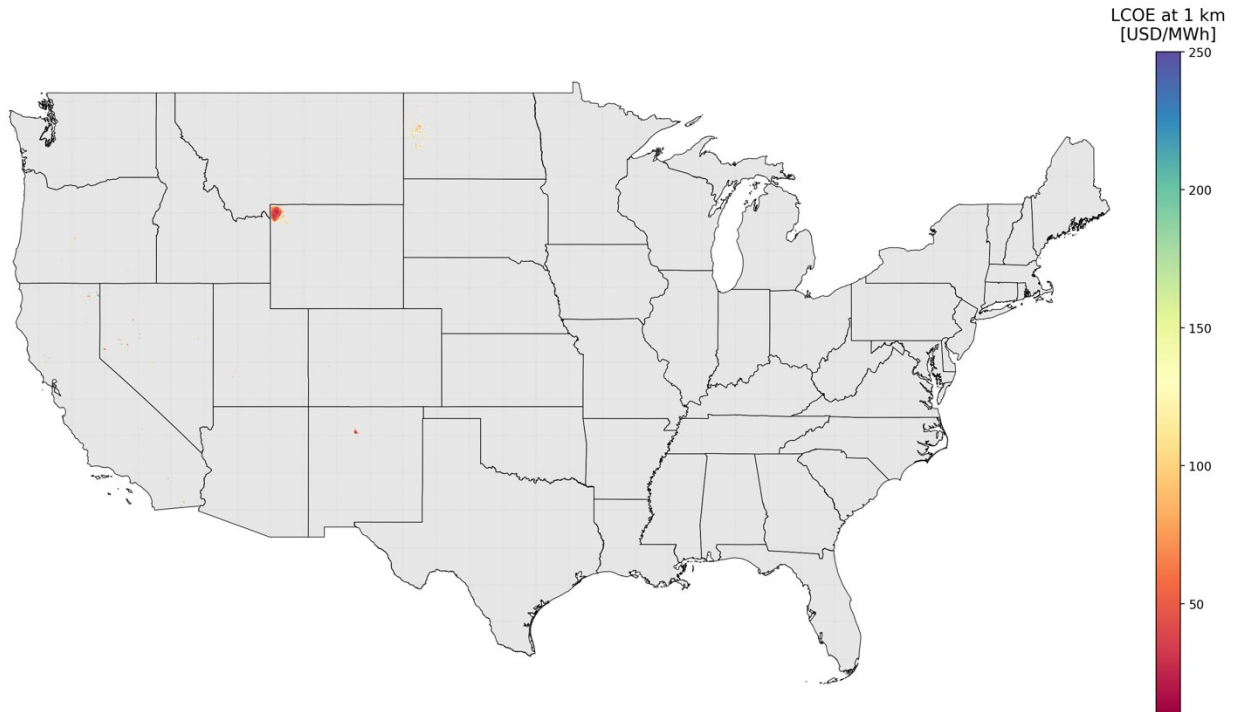


Figure A1: LCOE of EGS systems around the continental United States at depth of 1 km.

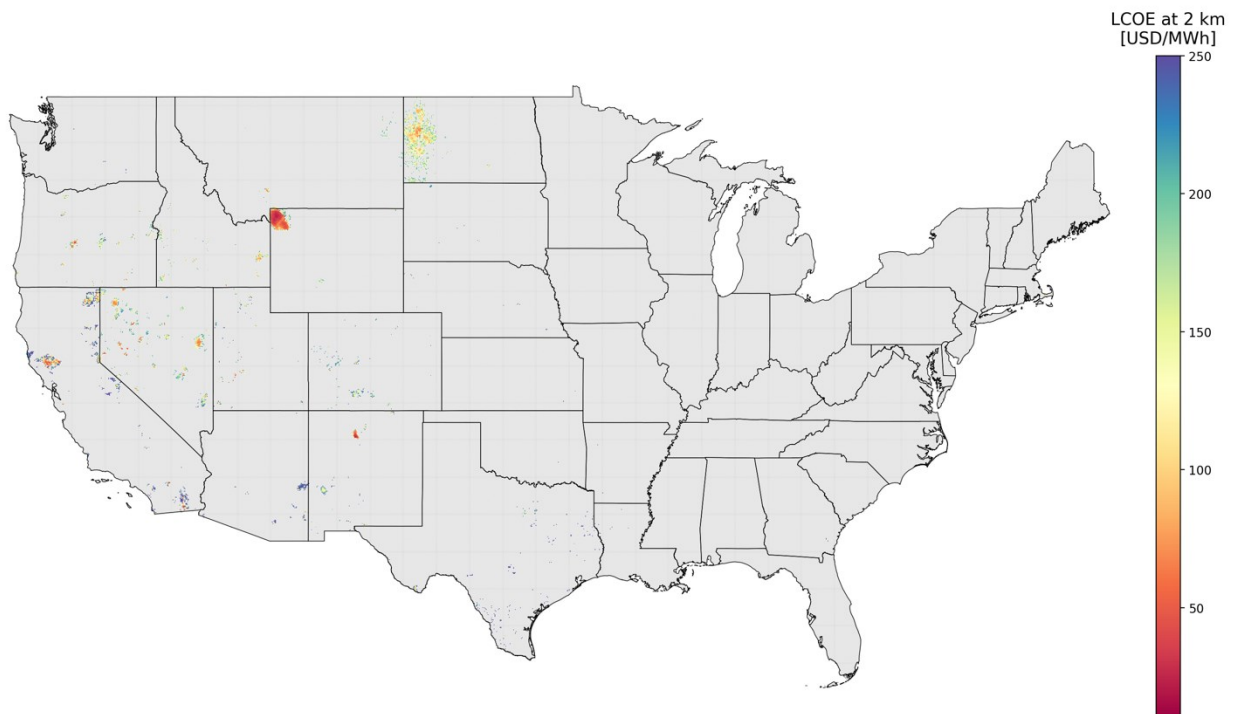


Figure A2: LCOE of EGS systems around the continental United States at depth of 2 km.

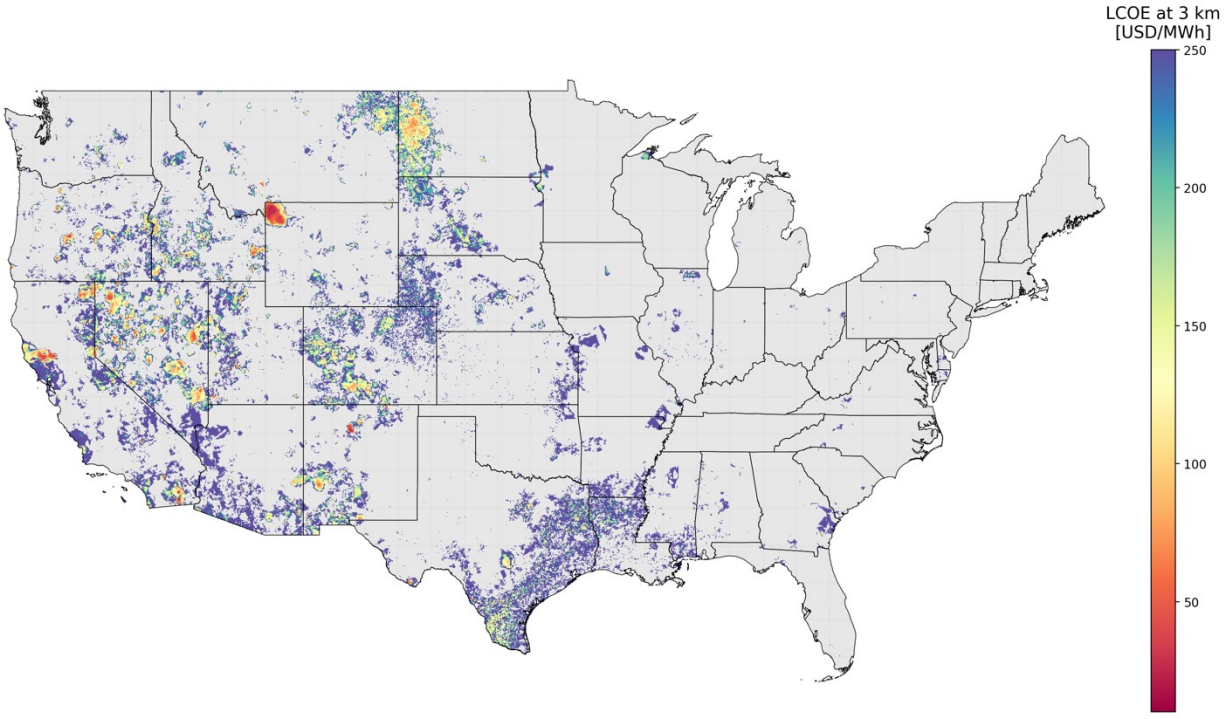


Figure A3: LCOE of EGS systems around the continental United States at depth of 3 km.

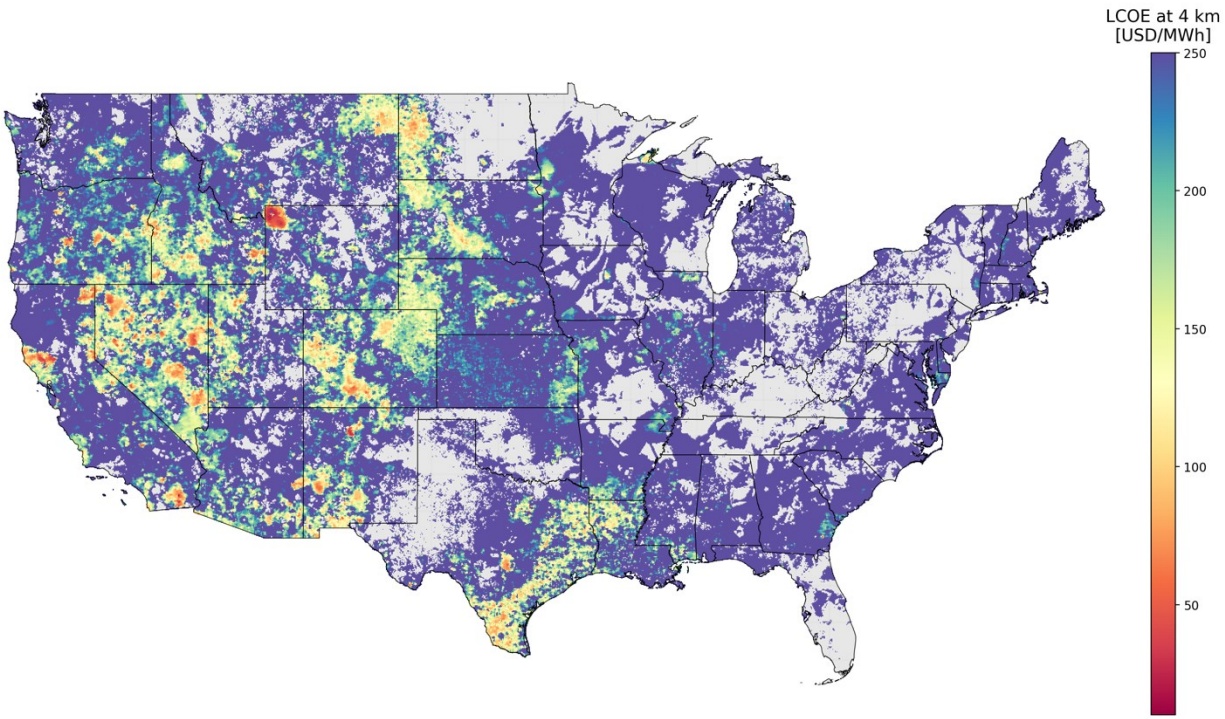


Figure A4: LCOE of EGS systems around the continental United States at depth of 4 km.

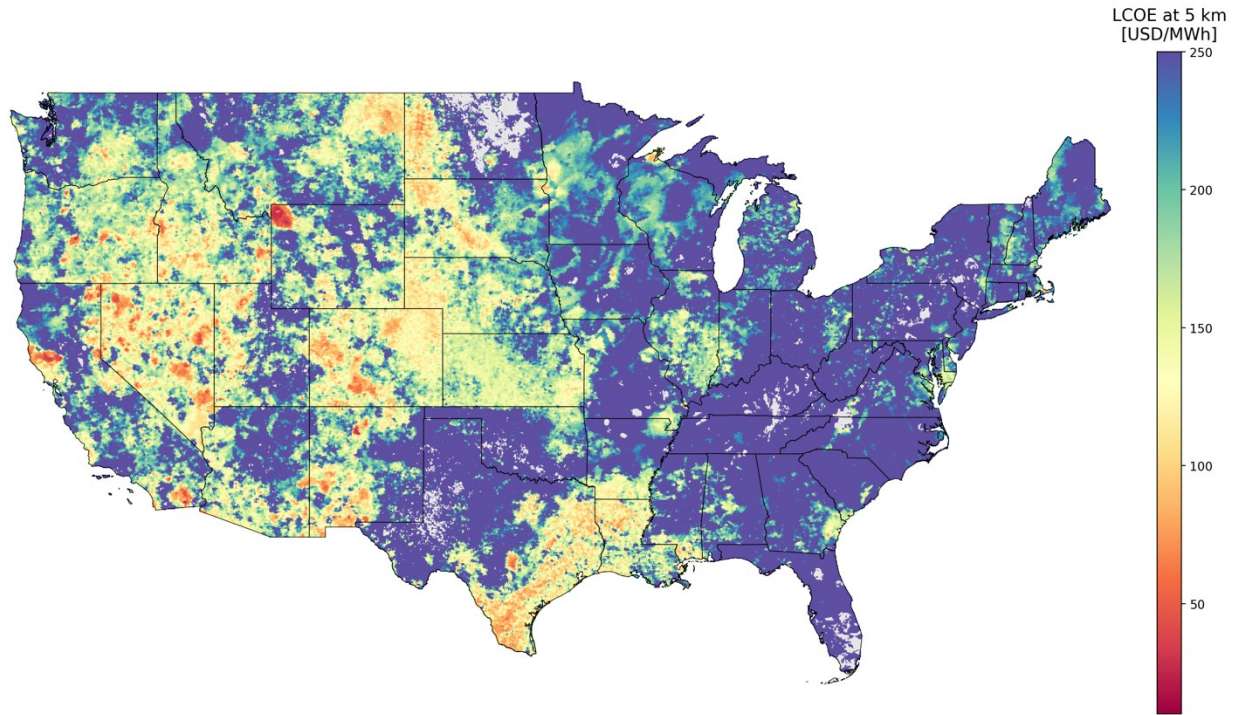


Figure A5: LCOE of EGS systems around the continental United States at depth of 5 km.

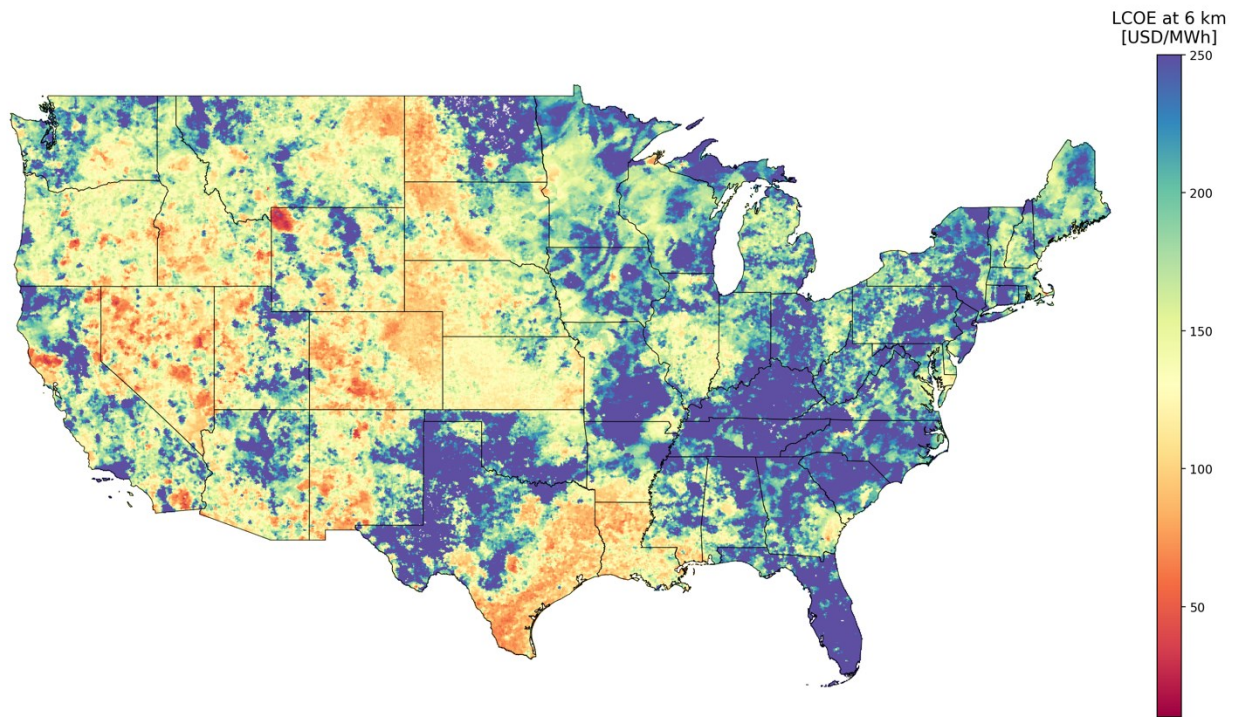


Figure A6: LCOE of EGS systems around the continental United States at depth of 6 km.

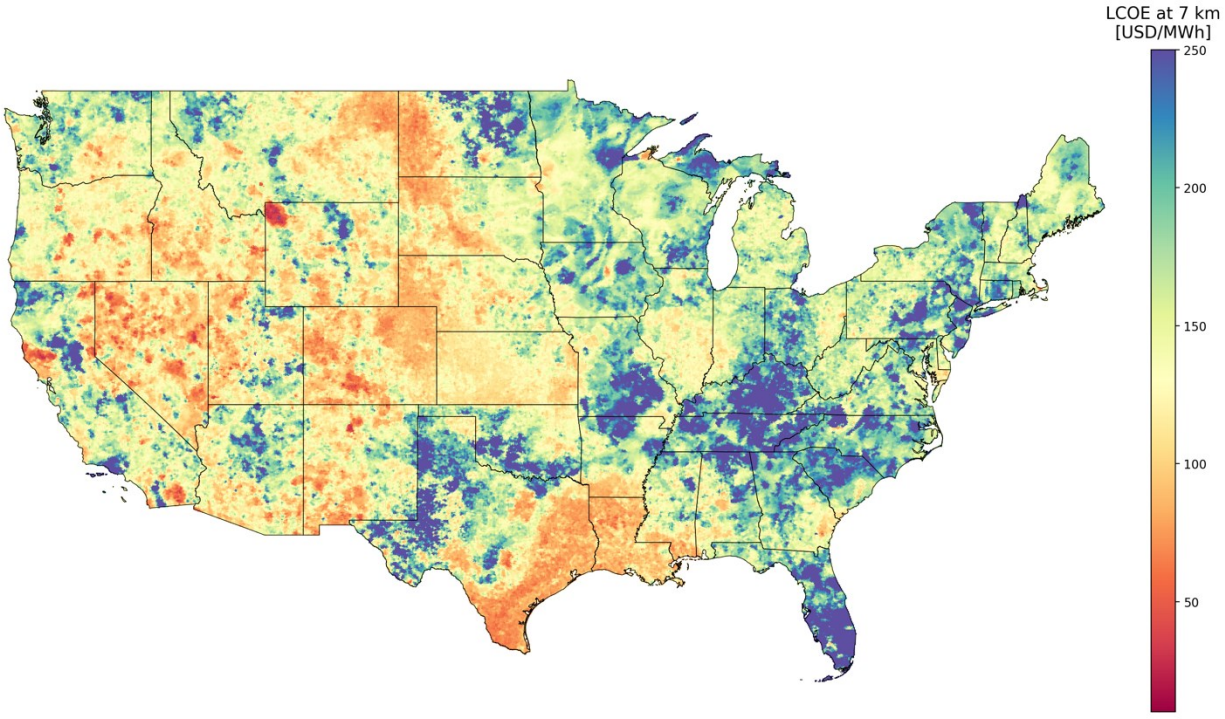


Figure A7: LCOE of EGS systems around the continental United States at depth of 7 km.